Stimulus-Responsive Materials

DOI: 10.1002/ange.201209299

Biomolecular Assembly of Thermoresponsive Superlattices of the Tobacco Mosaic Virus with Large Tunable Interparticle Distances**

Tao Li, Xingjie Zan, Randall E. Winans, Qian Wang, and Byeongdu Lee**

The fabrication of crystalline assemblies, or superlattices, of 1D nanoscale building blocks is of great interest because of the collective properties that may result from the uniform arrangement of the components. For these collective properties to be tuned, control over not only the symmetry of the building blocks but also the distance between them is crucial. Various assembly methods that utilize enthalpic or entropic interactions, such as solvent evaporation,[1] DNA base pairing,[2] or charge,[3] have been developed for the fabrication of superlattice structures, as well as strategies based on external magnetic[4] and electric forces.[5]

Recently, the depletion interaction has received considerable attention because it is a simple but powerful means to direct and control the self-assembly of anisotropic particles with tunable interparticle distances.[6] In brief, the depletion interaction between nanoparticles in a solution is invoked when additives, such as polymers or micelles, are present. The additives push the particles closer together through osmotic pressure and thus gain the free volume (Figure 1). The attractive depletion interaction induced by the depletant is often balanced by the repulsive electrostatic interaction due to the surface charge of the particles.[6a,b,7]

Herein, we show that a wide range of interparticle distances between rodlike particles are possible when rigid polymers are used as depletants; the lattice parameter, d, of the superlattice of rodlike particles can be tuned from approximately 1 to 5 times the diameter, D, of the rodlike particles. We found that the depletion interaction alone cannot explain these large interparticle distances and propose a second mechanism by which the polymers are able to induce self-assembly. Furthermore, we show that the interparticle distance can be controlled reversibly in response to external stimuli, such as temperature, if rigid gel-forming polymers are used.[8]

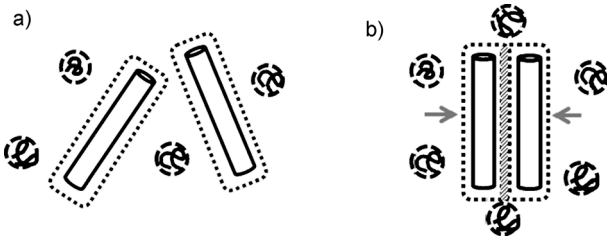

Figure 1. Origin of the depletion interaction. a) Rodlike particles mixed with depletants (dashed spheres). The mass center of the depletant is excluded from a shell around the rodlike particles. The shell, whose thickness is identical to the radius of the depletants, is called the depletion layer (dashed lines around the rods). b) By pushing the rods closer together through osmotic pressure (arrows), the depletants gain the free volume by reducing the inaccessible volume (shaded region). The strength of the effective attractive interaction, called the depletion interaction, between rods is proportional to the osmotic pressure and the overlapped volume of the depletion layers.

Rodlike tobacco mosaic virus (TMV) was chosen as a model 1D building block since it is well-known to assemble through the depletion interaction. TMV is a naturally occurring protein cage with a hollow cylindrical shape (ca. 18 nm in diameter, ca. 300 nm in length, and with a cavity diameter of ca. 4 nm; Figure 2a). Polysaccharides were chosen as depletants because they are often temperature-responsive and rigid; owing to their rigidity, polysaccharides can deplete TMV at a much lower concentration than that required for other additives.[6]

To better understand how polysaccharides behave as depletants, we first investigated the assembly of TMV with a representative rigid polysaccharide, sodium carboxymethyl cellulose (CMC; see Scheme S1 in the Supporting Information). We used small-angle X-ray scattering (SAXS)[2a,6e,9] so that we could study more than just the isotropic–nematic (I–N) phase boundary.

We performed a number of experiments in which we varied the polymer concentration. Because the osmotic pressure varies with the polymer concentration, the distance between TMV particles, d, should also vary with the polymer concentration (Figure 1).[10] In polymer physics, three concentration regimes, which depend on the extent to which the polymer chains overlap, should be considered: 1) In the dilute regime, each polymer chain is isolated. The osmotic pressure increases as the number of polymer molecules increases (as in

[*] Dr. T. Li,[+] Dr. R. E. Winans, Dr. B. Lee
X-ray Science Division, Argonne National Laboratory
9700 Cass Avenue, Lemont, IL 60439 (USA)
E-mail: blee@aps.anl.gov
Homepage: http://sites.google.com/site/byeongdu/home
Dr. X. Zan,[+] Prof. Q. Wang
Department of Chemistry and Biochemistry
University of South Carolina
Columbia, SC 29208 (USA)
E-mail: wang263@mailbox.sc.edu
Homepage: http://www.chem.sc.edu/faculty/wang/
[+] These authors contributed equally.

[**] T.L. and B.L. are thankful for the use of the Advanced Photon Source, an Office of Science User Facility operated for the US Department of Energy (DOE) Office of Science by Argonne National Laboratory; the use of this facility was supported by the US DOE under Contract No. DE-AC02-06CH11357. Q.W. is grateful for financial support from the US NSF (CHE-0748690), the US DSF (DMR-0706431), the US DoD (W911NF-09-1-0236), the US DOE (DE-SC0001477), and the W. M. Keck Foundation. We thank Dr. A. J. Senesi for helpful discussions.

Supporting information for this article is available on the WWW under http://dx.doi.org/10.1002/anie.201209299.

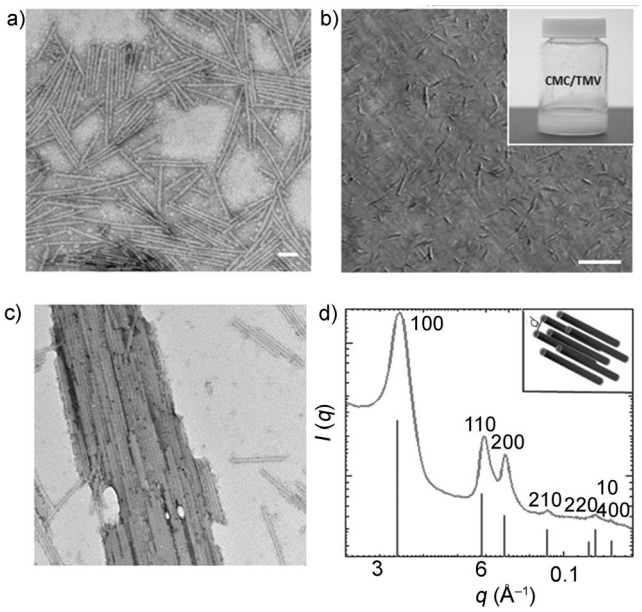

Figure 2. a) TEM image of TMV (dried without depletants). Scale bar: 100 nm. b) Optical microscopy image of a solution of TMV (15 mg mL^{-1}) containing CMC (4 wt%). Scale bar: 50 μm. The inset image shows the same sample. c) TEM image of the sample in (b). d) 1D SAXS curve of the sample in (b) indexed to a 2D hexagonal lattice. The distance between TMV particles, d, is calculated from the equation $d = 4\pi/\sqrt{3}q_{(100)}$.

Table 1: Physical parameters of the polymers used in this study.[a]

Polymer	M_w [kDa]	R_g [nm]	L_{p0} [nm]	L_{pe} [nm]	c^* [wt%]	c^{**} [wt%]
MC	210	23.4	15 ± 2[16]	0	0.42	4.5
CMC	250	48.6[17]	17 ± 2[17]	142.4[18]	0.02[19]	1.0[19]
PEO	200	22.6	< 1[20]	0	0.33	3.3

[a] M_w is the molecular weight of the polymer; R_g is the radius of gyration of the polymer; the persistence length of the polyelectrolyte is the sum of L_{p0}, the bare persistence length, and L_{pe}, the electrostatic contribution; c^* is the semidilute overlap concentration; c^{**} is the entanglement concentration, which separates the concentrated regime from the semidilute regime. The values c^* and c^{**} for MC and PEO were obtained from viscosity measurements (see Figure S9).

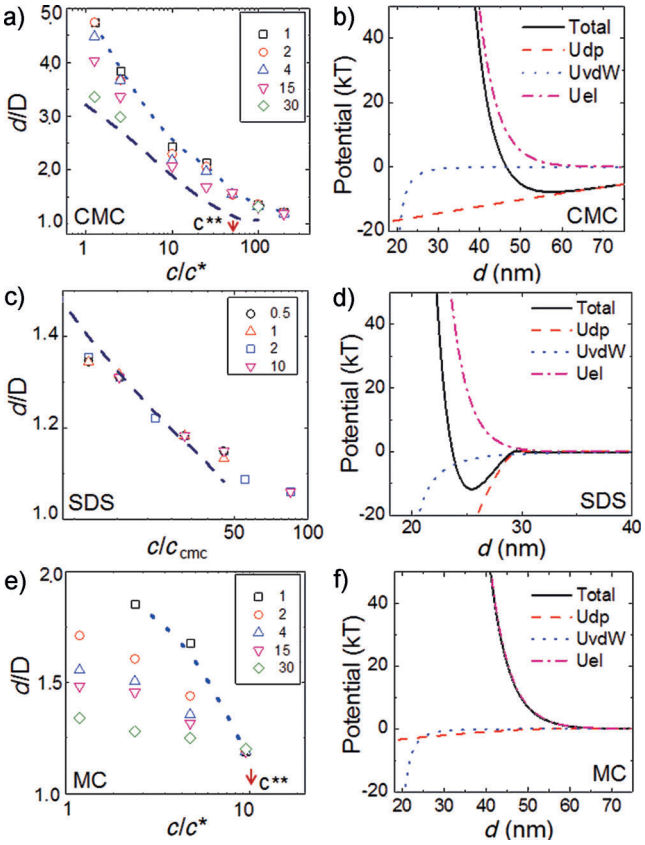

Figure 3. a,c,e) Relationship obtained from SAXS data between the ratio d/D and the concentration of the depletant for CMC, SDS, and MC. The corresponding TMV concentrations (unit: mg mL^{-1}) are given in the legend in each case. The dashed curve in (a) and (c) shows the theoretical d value calculated from pair potentials by balancing the depletion, van der Waals, and electrostatic interactions. The dotted curve in (a) and (e) represents the observed isotropic–nematic phase boundary. b,d,f) Pair potentials for CMC, SDS, and MC (the depletion, van der Waals, and electrostatic pair potentials are denoted *U*dp, *U*vdW, and *U*el, respectively). The concentrations of CMC, SDS, and MC are $c = c^*$, 3 wt%, and $c = c^*$, respectively.

an ideal solution), and each single chain behaves as a depletant. 2) In the semidilute regime, polymer chains overlap slightly. This overlap causes repulsive interchain interactions and consequently leads to higher osmotic pressure than that predicted by the Raoult law. Polyelectrolytes, such as CMC, will incur higher osmotic pressure than neutral polymers since their chains repel each other not only sterically but also electrostatically (see the Supporting Information). 3) Finally, in the concentrated regime, in which polymer chains are entangled, individual chains are not discernible, and the osmotic pressure is drastically increased relative to that in the semidilute regime.[10] In both the semidilute and concentrated regimes, the interchain distance is defined as the correlation length (ξ). Under these conditions, a blob with the size of the correlation length functions as a depletant, instead of the entire polymer chain.[11] The boundaries between concentration regimes (1) and (2) and between regimes (2) and (3) are denoted as the overlap (c^*) and entanglement concentration (c^{**}), respectively. Table 1 lists the c^* and c^{**} values of the polymers used in this study, as determined from viscosity measurements (see the Supporting Information). Details about the osmotic pressure and correlation length can be found in the Supporting Information and Ref. [10]. The distribution of polymer chains in these three regimes is depicted in Figure 4.

We found unique TMV self-assembly behavior in each of these three regimes. Without CMC, the solution of TMV was clear, and SAXS profiles showed only the form factor scattering without any diffraction peaks. These observations indicate that TMV exists as an isotropic phase (see Figure S1 in the Supporting Information). At high concentrations of CMC (concentrated regime), the sample became opaque. Optical microscopy (Figure 2b) and TEM (Figure 2c) of a sample with 4 wt% (c/c* ≈ 200) of CMC confirmed that the turbidity is due to the formation of TMV bundles. SAXS analysis of the same sample in solution (Figure 2d) showed seven sharp diffraction peaks whose positions were in good

agreement with the ideal diffraction pattern of a 2D hexagonal lattice.[2a,12]

Superlattice formation was observed not only in the concentrated regime (or for dried samples; $c > c^{**}$) but also in the semidilute regime ($c^* < c < c^{**}$; Figure 3a; see also Figures S2 and S3). The observed I–N phase boundary is consistent with theory and other experimental observations:

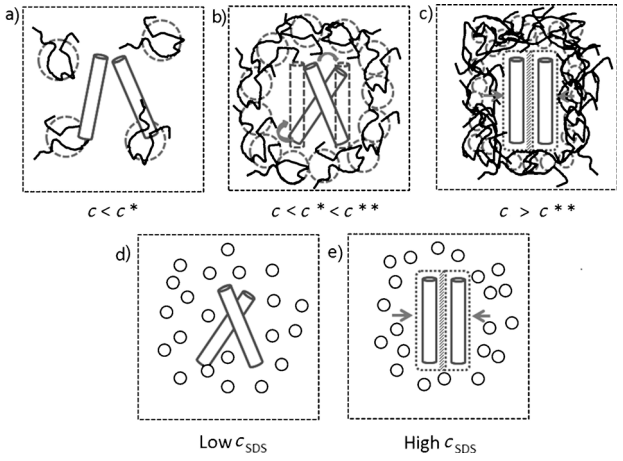

Figure 4. Schematic illustration of TMV particles in the a) dilute, b) semidilute, and c) concentrated regimes of the polymer, as well as at d) low and e) high concentrations of SDS. The dashed circles in (a–c) represent the correlation length. The shaded volumes in (c) and (e) are the volumes each depletant will gain by compressing the TMV domain.

TMV aggregates as the concentration of either the polymer or TMV increases.[7a,13] Surprisingly, the nearest-neighbor distance, d, or the lattice parameter, close to the boundary was as large as 85.4 nm, which is approximately 5 times the diameter, D, of TMV (18 nm). The d/D value was much larger than other values reported previously.[6a,b,7a] As the concentration decreased below c^{**}, the d/D value started to deviate from the theoretical value predicted by balancing the depletion, van der Waals, and electrostatic pair potentials (Figure 3b; see also the Supporting Information).[6e,7a,14] In other words, in the semidilute regime, d is dependent on the particle concentration (Figure 3a). These results indicate that in the semidilute concentration regime, CMC does not behave solely as a depletant.

To better understand the role of CMC as a depletant, we compared CMC with a standard depletant, sodium dodecyl sulfate (SDS) micelles, which have been modeled as small hard spheres.[6e] SDS micelles also caused TMV to aggregate into a 2D hexagonal superlattice (see Figures S4 and S5). The observed d values decreased with the SDS concentration (Figure 3c) and matched the values calculated by balancing pair potentials very well (Figure 3d). In contrast to the CMC/TMV system, the SDS/TMV system was not dependent on the TMV concentration for the entire range of SDS concentrations studied. This observation further suggests that CMC introduces an additional type of interaction other than just the depletion interaction in the semidilute concentration regime (Figure 3a; see also the Supporting Information).

We hypothesized that this new interaction results from the rigidity of the polymer: CMC can be considered a collection of large rigid rodlike segments, whereas SDS can be modeled as a small hard sphere. The rigidity of a polymer is defined by the persistence length, which corresponds to the length of its straight segment. We investigated the role of the persistence length on the assembly of TMV by using two additional polymers, methyl cellulose (MC) and poly(ethylene oxide) (PEO). MC and PEO have similar molecular weights and radii of gyration (Table 1) and will therefore evoke depletion interactions of similar strength. Additionally, they are both neutral polymers. The two polymers differ mainly in their persistence length. The persistence length of MC, a polysaccharide, is much longer than that of PEO, although it is about 10 times shorter than that of CMC.

The depletion interaction caused by these two neutral polymers is very low relative to that observed for CMC and SDS micelles (Figure 3f) because neutral polymers exert much lower osmotic pressure than polyelectrolytes.[10] No diffraction peak was observed when PEO (200 kDa) was added at concentrations up to 80 mg mL^{-1} ($c/c^* \approx 24$: concentrated regime) to a solution of TMV; thus, no assembly of TMV was detected. Surprisingly, MC induced assembly even though one would not expect its depletion attraction to counteract the electrostatic repulsion (there is no minimum in the pair-potential calculation in Figure 3f). As in the CMC/TMV system, the interparticle distance, d, in the MC/TMV system is dependent on the TMV concentration within the semidilute regime ($c^* < c < c^{**}$), and it becomes independent at $c > c^{**}$ (Figure 3e). This result indicates that the mechanism through which MC induces assembly is similar to that for CMC/TMV at low TMV (below ca. 30 mg mL^{-1}) and CMC concentrations ($c < c^{**}$; Figure 3a), and that the persistence length plays a critical role in the induction of assembly by polymers. Furthermore, the maximum d value for the MC/TMV system is significantly smaller than that for the CMC/TMV system. In other words, MC (which has a shorter persistence length) gives rise to significantly weaker interactions than those promoted by CMC (which has a longer persistence length).

The role of the persistence length in the assembly process can be deduced from the results of studies by Onsager:[15] rodlike particles may align parallel to one another as in liquid crystals at a concentration as low as 5 vol% without any depletants, since they occupy less volume when they are aligned than when they are randomly arranged (in other words, each particle gains more free volume). Although the system may lose entropy as a result of the ordering, the gain in free-volume entropy is enough to compensate the loss.

The concentration of TMV in this study was below 3 vol%. However, the total concentration of rods is much greater if one considers both TMV and CMC as rodlike particles. When these rods (TMV particles and the rigid sections of the polymers) are randomly arranged, there will be volume that is sterically inaccessible to both TMV and the polymer (such as the regions between the two rods packed at a random angle in Figure 4b). When the rods are rearranged and aligned parallel to each other, the system gains free-volume entropy (Figure 4b). Conversely, these regions are

accessible to small depletants; therefore, the free-volume gain is not expected when SDS is used as a depletant (Figure 4d,e). PEO cannot trigger the alignment of TMV particles either, since it does not have a rodlike unit and the penalty associated with the wrapping of its chain around TMV is lower than for its rigid counterparts. The observation that the onset of assembly formation is at $c \approx c^*$, a concentration at which polymer chains occupy the entire volume of the solution, suggests that TMV particles assemble because they are confined in the small space left over by the polymer chains (Figure 4b). Therefore, the role of rigid polymers in this free-volume-entropy mechanism is twofold: they confine the TMV particles (but do not press them together) and trigger the assembly. The distance d decreases as the TMV concentration increases in this regime because there are more TMV particles in the same confined space.

As the concentration of the polymer increases, the depletion mechanism plays a larger role in superlattice formation, and the free-volume effect disappears (Figure 4c). The cross-over concentration between the two mechanisms is located near c^{**}. We hypothesize that this finding is related to the degree of entanglement of the polymer chains. As polymer chains become entangled, the steric repulsion between the chains increases drastically, and the confined space (Figure 4b) is reduced to the point that the TMV superlattice can no longer be compressed further. As a result, TMV will be closed packed ($d/D \approx 1$), regardless of its concentration. At extremely high concentrations of the polymer ($c \gg c^{**}$), or for dried samples, the d/D value becomes less than 1, because each TMV is itself dehydrated (data not shown).

The significantly larger d values observed with CMC/TMV than with MC/TMV are a result of the combination of two mechanisms. First, CMC is a polyelectrolyte and therefore invokes a much stronger osmotic pressure than MC (see dashed line in Figure 3a).[10] Furthermore, its long persistence length enables the free-volume gain, and therefore TMV can align at concentrations (of the polymer or particles) lower than that required for the depletion interaction. Through these two mechanisms, the maximum d/D value of the CMC/TMV system is as high as approximately 5.

One notable property of MC is that it can form physical gels when heated above a critical temperature. This behavior suggests that MC could act as a temperature-responsive medium to trigger the assembly or disassembly of colloidal particles. When the polymer goes through the sol-to-gel transition as the temperature increases, the second virial coefficient, A_2, of the polymer changes from positive to negative, which means that the solubility of the polymer becomes poor: A_2 is positive when the polymer is soluble and is negative when the polymer is insoluble. In other words, MC releases water to its surroundings (in the sol-to-gel transition) or attracts water from its surroundings (in the gel-to-sol transition).[21] The polymer chains expand or shrink as A_2 becomes positive (sol) or negative (gel), respectively. The released water hydrates the TMV superlattice and thus leads to an increase in the interparticle distance d. Conversely, the superlattice contracts as the polymer becomes a sol and removes water from the TMV assembly. Both the reversible variation of d and assembly/disassembly behavior were observed experimentally (Figure 5a–c). It is also possible to reverse the temperature dependency so that TMV disassembles (or the lattice expands) at a lower temperature and assembles (or the lattice contracts) at a higher temperature by the use of other polysaccharides, such as κ-carrageenan (KC; see Scheme S1 in the Supporting Information), which forms a gel at a lower temperature and a sol at a higher temperature.[22] Figure 5d,e shows the reversible variation of the d value of a TMV superlattice embedded in KC, whereby d decreases with increasing temperature. Since KC has a longer persistence length,[23] the observed d values span a wider range in response to temperature than those found with MC.

In summary, we have demonstrated that TMV nanorods mixed with polymers or micelles can form a superlattice through a combination of the depletion interaction (d is not

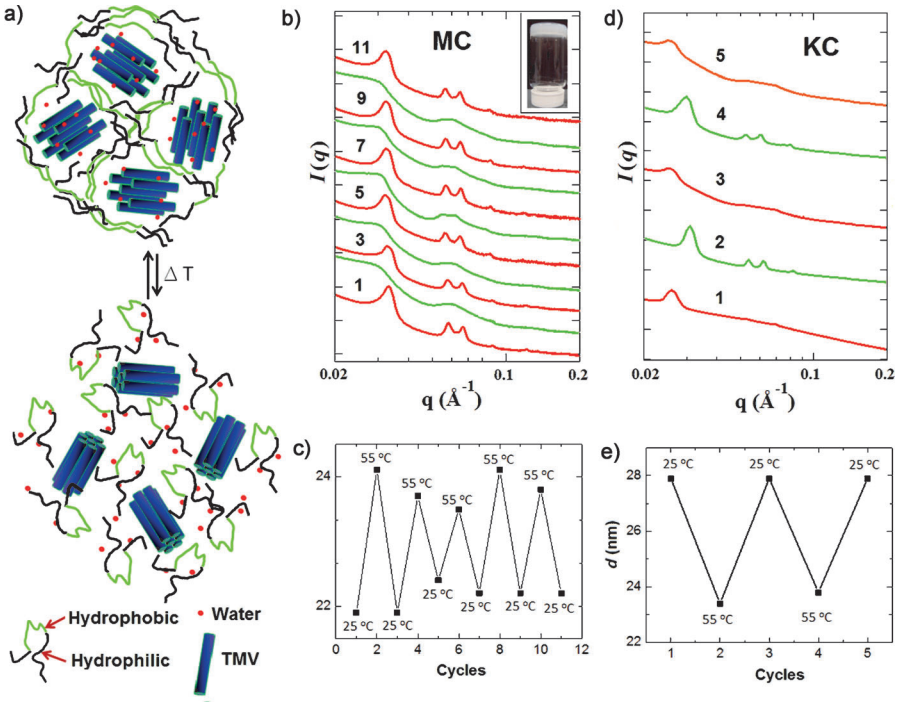

Figure 5. a) Schematic representation of the polysaccharide/TMV sol–gel transition. MC and KC form a gel through a hydrophobic interaction. b,d) SAXS curves for the samples containing MC (4 wt%) with TMV at a concentration of 15 mg mL^{-1} (b) and KC (3 wt%) with TMV at a concentration of 2 mg mL^{-1} (d) at various temperatures shown in (c) and (e) during heating/cooling cycles. The SAXS data in (b) and (d) are offset for clarity. At 25 °C, MC and KC are a sol and a gel, respectively, and at 55 °C, they are in their opposite states. The inset image in (b) shows the sample in a gel state at 45 °C.

dependent on the TMV concentration) and a free-volume gain (d varies with the TMV concentration). The latter mechanism is significant when the polymer is rigid and the polymer solution is in the semidilute regime. These mechanisms yield a superlattice with a wide range of lattice parameters up to 5 times the diameter of the particles; such large lattice parameters cannot be attained with other types of depletants. Furthermore, we showed that the lattice parameter of the superlattice can be controlled reversibly in response to external stimuli; it can expand or contract upon changes in temperature, depending on the type of gel-forming polymer employed. This simple, yet powerful method enables the production of stimulus-responsive materials with potential applications in many fields.[24]

Received: November 20, 2012
Revised: March 15, 2013
Published online: May 16, 2013

Keywords: depletion force · self-assembly · stimulus-responsive materials · superlattices · viruses

[1] a) Y. Lin, E. Balizan, L. A. Lee, Z. W. Niu, Q. Wang, *Angew. Chem.* **2010**, *122*, 880 – 884; *Angew. Chem. Int. Ed.* **2010**, *49*, 868 – 872; b) E. V. Shevchenko, D. V. Talapin, N. A. Kotov, S. O'Brien, C. B. Murray, *Nature* **2006**, *439*, 55 – 59.

[2] a) M. R. Jones, R. J. Macfarlane, B. Lee, J. Zhang, K. L. Young, A. J. Senesi, C. A. Mirkin, *Nat. Mater.* **2010**, *9*, 913 – 917; b) P. Cigler, A. K. R. Lytton-Jean, D. G. Anderson, M. G. Finn, S. Y. Park, *Nat. Mater.* **2010**, *9*, 918 – 922; c) S. Y. Park, A. K. Lytton-Jean, B. Lee, S. Weigand, G. C. Schatz, C. A. Mirkin, *Nature* **2008**, *451*, 553 – 556; d) D. Nykypanchuk, M. M. Maye, D. van der Lelie, O. Gang, *Nature* **2008**, *451*, 549 – 552.

[3] a) H. G. Cui, E. T. Pashuck, Y. S. Velichko, S. J. Weigand, A. G. Cheetham, C. J. Newcomb, S. I. Stupp, *Science* **2010**, *327*, 555 – 559; b) A. M. Kalsin, M. Fialkowski, M. Paszewski, S. K. Smoukov, K. J. M. Bishop, B. A. Grzybowski, *Science* **2006**, *312*, 420 – 424.

[4] a) H. Kim, J. Ge, J. Kim, S. Choi, H. Lee, H. Lee, W. Park, Y. Yin, S. Kwon, *Nat. Photonics* **2009**, *3*, 534 – 540; b) J. P. Ge, Y. X. Hu, Y. D. Yin, *Angew. Chem.* **2007**, *119*, 7572 – 7575; *Angew. Chem. Int. Ed.* **2007**, *46*, 7428 – 7431.

[5] a) S. Gupta, Q. L. Zhang, T. Emrick, T. P. Russell, *Nano Lett.* **2006**, *6*, 2066 – 2069; b) K. M. Ryan, A. Mastroianni, K. A. Stancil, H. T. Liu, A. P. Alivisatos, *Nano Lett.* **2006**, *6*, 1479 – 1482.

[6] a) D. Baranov, A. Fiore, M. van Huis, C. Giannini, A. Falqui, U. Lafont, H. Zandbergen, M. Zanella, R. Cingolani, L. Manna, *Nano Lett.* **2010**, *10*, 743 – 749; b) E. Barry, Z. Dogic, *Proc. Natl. Acad. Sci. USA* **2010**, *107*, 10348 – 10353; c) S. Sacanna, W. T. M. Irvine, P. M. Chaikin, D. J. Pine, *Nature* **2010**, *464*, 575 – 578; d) J. Henzie, M. Grünwald, A. Widmer-Cooper, P. L. Geissler, P. Yang, *Nat. Mater.* **2012**, *11*, 131 – 137; e) K. L. Young, M. R. Jones, J. Zhang, R. J. Macfarlane, R. Esquivel-Sirvent, R. J. Nap, J. Wu, G. C. Schatz, B. Lee, C. A. Mirkin, *Proc. Natl. Acad. Sci. USA* **2012**, *109*, 2240; f) P. F. Damasceno, M. Engel, S. C. Glotzer, *Science* **2012**, *337*, 453 – 457.

[7] a) M. Imai, N. Urakami, A. Nakamura, R. Takada, R. Oikawa, Y. Sano, *Langmuir* **2002**, *18*, 9918 – 9923; b) N. Urakami, M. Imai, Y. Sano, M. Takasu, *J. Chem. Phys.* **1999**, *111*, 2322 – 2328.

[8] a) M. A. Cohen Stuart, W. T. S. Huck, J. Genzer, M. Müller, C. Ober, M. Stamm, G. B. Sukhorukov, I. Szleifer, V. V. Tsukruk, M. Urban, F. Winnik, S. Zauscher, I. Luzinov, S. Minko, *Nat. Mater.* **2010**, *9*, 101 – 113; b) R. J. Wojtecki, M. A. Meador, S. J. Rowan, *Nat. Mater.* **2011**, *10*, 14 – 27; c) M. A. Kostiainen, C. Pietsch, R. Hoogenboom, R. J. M. Nolte, J. J. L. M. Cornelissen, *Adv. Funct. Mater.* **2011**, *21*, 2012 – 2019.

[9] R. J. Macfarlane, B. Lee, M. R. Jones, N. Harris, G. C. Schatz, C. A. Mirkin, *Science* **2011**, *334*, 204 – 208.

[10] R. H. Colby, *Rheol. Acta* **2010**, *49*, 425 – 442.

[11] R. Verma, J. C. Crocker, T. C. Lubensky, A. G. Yodh, *Phys. Rev. Lett.* **1998**, *81*, 4004 – 4007.

[12] T. Li, R. E. Winans, B. Lee, *Langmuir* **2011**, *27*, 10929 – 10937.

[13] a) H. Graf, H. Löwen, *Phys. Rev. E* **1999**, *59*, 1932 – 1942; b) M. Adams, S. Fraden, *Biophys. J.* **1998**, *74*, 669 – 677.

[14] S. Asakura, F. Oosawa, *J. Polym. Sci.* **1958**, *33*, 183 – 192.

[15] a) H. N. W. Lekkerkerker, R. Tuinier in *Colloids and the Depletion Interaction*, Springer, Berlin, **2011**; b) S. Fraden, G. Maret, D. L. D. Caspar, *Phys. Rev. E* **1993**, *48*, 2816 – 2837; c) L. Onsager, *Ann. N. Y. Acad. Sci.* **1949**, *51*, 627 – 659.

[16] T. R. Patel, G. A. Morris, J. G. de La Torre, A. Ortega, P. Mischnick, S. E. Harding, *Macromol. Biosci.* **2008**, *8*, 1108 – 1115.

[17] C. W. Hoogendam, A. de Keizer, M. A. C. Stuart, B. H. Bijsterbosch, J. A. M. Smit, J. A. P. P. van Dijk, P. M. van der Horst, J. C. Batelaan, *Macromolecules* **1998**, *31*, 6297 – 6309.

[18] M. Tricot, *Macromolecules* **1984**, *17*, 1698 – 1704.

[19] Q. Wu, Y. Shangguan, M. Du, J. Zhou, Y. Song, Q. Zheng, *J. Colloid Interface Sci.* **2009**, *339*, 236 – 242.

[20] S. Kawaguchi, G. Imai, J. Suzuki, A. Miyahara, T. Kitano, K. Ito, *Polymer* **1997**, *38*, 2885 – 2891.

[21] T. Kato, M. Yokoyama, A. Takahashi, *Colloid Polym. Sci.* **1978**, *256*, 15 – 21.

[22] a) Y. Yuguchi, T. T. Thu Thuy, H. Urakawa, K. Kajiwara, *Food Hydrocolloids* **2002**, *16*, 515 – 522; b) M. Tomšič, F. Prossnigg, O. Glatter, *J. Colloid Interface Sci.* **2008**, *322*, 41 – 50.

[23] F. Cuppo, H. Reynaers, S. Paoletti, *Macromolecules* **2001**, *35*, 539 – 547.

[24] a) E. S. Gil, S. M. Hudson, *Prog. Polym. Sci.* **2004**, *29*, 1173 – 1222; b) C. J. Murphy, T. K. San, A. M. Gole, C. J. Orendorff, J. X. Gao, L. Gou, S. E. Hunyadi, T. Li, *J. Phys. Chem. B* **2005**, *109*, 13857 – 13870; c) Z. Huang, H. Lee, E. Lee, S.-K. Kang, J.-M. Nam, M. Lee, *Nat. Commun.* **2011**, *2*, 459; d) C. Weber, R. Hoogenboom, U. S. Schubert, *Prog. Polym. Sci.* **2012**, *37*, 686 – 714.

